



Optical vortex generation in homeotropic NLCs in the presence of DC electric field

I. A. Budagovsky, S. A. Shvetsov & A. S. Zolot'ko

To cite this article: I. A. Budagovsky, S. A. Shvetsov & A. S. Zolot'ko (2016) Optical vortex generation in homeotropic NLCs in the presence of DC electric field, Molecular Crystals and Liquid Crystals, 637:1, 47-52, DOI: [10.1080/15421406.2016.1198663](https://doi.org/10.1080/15421406.2016.1198663)

To link to this article: <http://dx.doi.org/10.1080/15421406.2016.1198663>



Published online: 10 Nov 2016.



Submit your article to this journal [↗](#)



Article views: 13



View related articles [↗](#)



View Crossmark data [↗](#)

Optical vortex generation in homeotropic NLCs in the presence of DC electric field

I. A. Budagovsky^a, S. A. Shvetsov^{a,b}, and A. S. Zolot'ko^a

^aLebedev Physical Institute, Moscow, Russia; ^bMoscow Institute of Physics and Technology, Dolgoprudny, Moscow Region, Russia

ABSTRACT

The generation of optical vortices in nematic liquid crystals (NLCs) due to the photorefractive effect has been studied. The vortices can appear in the NLCs with both positive and negative dielectric anisotropy. The efficiency of the Gaussian beam (TEM_{00}) to vortex conversion approached about 30%.

KEYWORDS



Nematic liquid crystal;
Optical vortex;
Photorefractive effect

Introduction

Optical vortices, i.e., light beams with orbital angular momentum, are of great interest due to their importance for both the fundamental optics and various applications, e.g., trapping and manipulation of microparticles [1,2]. One approach to the optical vortex generation consists in passing a Gaussian light beam (TEM_{00}) through an axially symmetric anisotropic structure [3,4]. Such structures can occur in nematic liquid crystals (NLCs), which represent a strongly anisotropic medium highly sensitive to external agents. The axially symmetric distributions of the director field can exist in nematic droplets [5] or be formed, e.g., by photoalignment [3], a torque due to highly focused light beam [6], or a director reorientation in the region of the nematic–isotropic phase transition due to laser heating [7]. In [8,9], optical vortices were obtained using a light valve, i.e., a homeotropic NLC with photoconductive layer. In [10], the generation of optical vortices due to the photorefractive effect [11,12] was first demonstrated by an example of an NLC with the positive dielectric anisotropy. In this paper, we report the results of the investigation of the optical vortex generation in NLCs with both signs of the dielectric anisotropy.

Experimental

When a dc voltage is applied to an NLC, the field is screened, at least partially, by ions at the NLC–substrate interface. A light wave incident on an NLC removes screening, mostly on the anode surface, and the dc electric field penetrates into the NLC bulk and results in the director reorientation (the effect of light is independent of the light polarization). For a spatially limited light beam, as shown in [12] by an example of the light beam self-action, the transversely inhomogeneous dc field can be approximated by the field of a point charge

CONTACT I. A. Budagovsky  v_brz@mail.ru  P. N. Lebedev Physics Institute, Russian Academy of Sciences, Leninsky prosp. 53, 119991 Moscow, Russia.

Color versions of one or more of the figures in the article can be found online at www.tandfonline.com/gmcl.

© 2016 Taylor & Francis Group, LLC

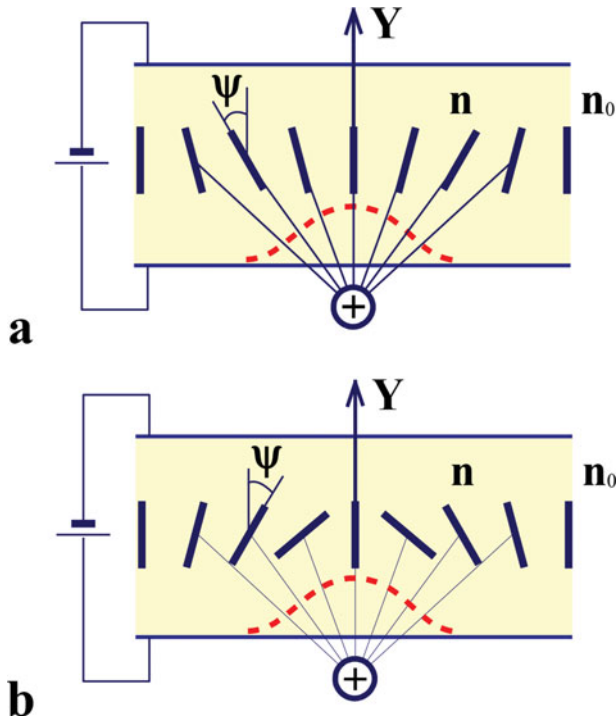


Figure 1. Director reorientation in NLCs under the action of the electric field penetrating into the NLC bulk due to the elimination of the screening by surface charges for (a) the positive and (b) negative dielectric anisotropy. The light beam axis coincides with the Y axis; the light beam intensity profile is shown by dashed curve; the penetrating electric field is simulated by that of the point charge; \mathbf{n}_0 is the unperturbed director; \mathbf{n} is the rotated director; and ψ is the director rotation angle.

located outside the nematic layer. The director distributions in the homeotropic NLCs with the positive and negative dielectric anisotropy produced by such a charge are shown in Fig. 1. In both cases, the director field is axially symmetric. For the positive dielectric anisotropy, the director orientation is limited by the field lines of the electric charge. For the negative dielectric anisotropy, the NLC director rotates away from the electric field and the angle of the director rotation can be larger. However, the orientation of the director on the beam axis (the Y axis in Fig. 1) can be destabilized in this case, in contrast to the positive dielectric anisotropy.

The director rotation by an angle $\psi(y, \rho)$ (ρ is the distance of a point from the Y axis) results in the phase shift between the extraordinary and ordinary waves

$$S(\rho) = k\Delta n \int_0^L \sin^2 \psi(y, \rho) dy, \quad (1)$$

where $k = 2\pi/\lambda$ is the light wave vector, λ is the light wavelength, Δn is the optical anisotropy, and L is the nematic layer thickness. If a circularly polarized Gaussian beam is incident on the NLC, the transmitted beam is (see, e.g., [7])

$$\begin{aligned} \mathbf{E}(R, \alpha) = & \frac{A_0 k w_0^2}{id} e^{\frac{ikR^2}{2d}} \int_0^\infty u e^{-u^2 + iS(u)/2} \{ \mathbf{e}_\pm \cos(S(u)/2) J_0(\tau u) \\ & - i \mathbf{e}_\mp e^{\pm 2i\alpha} \sin(S(u)/2) J_2(\tau u) \} du, \end{aligned} \quad (2)$$

where A_0 and w_0 are the amplitude and waist of the incident Gaussian (TEM_{00}) beam, \mathbf{e}_\pm is the unit vector of the incident circular polarization, R and α are the polar coordinates in the observation plane situated at a distance d from NLC, $\tau = kw_0R/d$, and $u = \rho/w_0$. The transmitted radiation is thus a sum of the non-vortex component (corresponding to the first term in braces) and the vortex component (the second term in braces). The vortex component has the circular polarization of the opposite sense with respect to the non-vortex component. The energy of the incident beam is distributed among the vortex and the non-vortex components having opposite senses of circular polarization. The efficiency η of the Gaussian beam to vortex conversion depends on the amplitude and profile of the phase shift $S(\rho)$, as well as on the beam waist.

The experimental samples were two homeotropically aligned cells filled with nematic materials (NIOPIK, Russia) with different signs of low-frequency dielectric anisotropy $\Delta\epsilon$: (1) ZhKM-1277 with $\Delta\epsilon = +12.3$ and (2) F-3 with $\Delta\epsilon = -0.5$. The thicknesses of the samples were, respectively, 100 and 25 μm ; the optical anisotropies of the materials were $\Delta n = 0.19$ and 0.1. The nematic-isotropic transition temperatures for both materials were above 60°C. The experiments were performed at room temperature. The glass plates of the cells were coated with ITO electrodes. The polarity of the applied dc voltage was taken as positive if the light beam was incident on the anode.

The homeotropic alignment of the cells was obtained using chromium stearyl chloride (CSC) orientant. Our previous experiments showed that incorporation of the “mordant pure yellow” dye (MPE) (Fig. 2) into the polyimide orientant (which was used to obtain the planar alignment) allows one to avoid the weakening of the photorefractive effect under long action of dc field probably due to the replenishment of the charge carriers in the NLC bulk. The same effect was found for the CSC orientant. For this reason, the substrates of the F-3 sample, for which the experimental data presented below were obtained, were coated with a mixture of CSC and MPE. At the same time, we noticed no substantial difference in the effects observed in the F-3 samples with and without MPE, if the time of dc voltage application was less than half an hour.

The schematic diagram of the experimental setup to generate optical vortices is shown in Fig. 3. The plane of the drawing corresponds to the vertical one. The direction of the linearly polarized radiation from a cw solid-state laser ($\lambda = 532$ nm, TEM_{00}) could be changed by a double Fresnel rhomb. The quarter wave plane allowed us to obtain the circularly polarized radiation. Then, the light beam was focused by a lens (the focal length was 15 cm) to the NLC cell. An additional quarter wave plate was used to transform the circular polarizations of the non-vortex and vortex components to the mutually perpendicular linear polarizations. When rotating the analyzer, we could observe on the screen the individual components or their interference. The angle β of the analyzer rotation was measured relative to the vertical plane. The conversion efficiency η was estimated as the ratio of the vortex component power to the total beam power measured after the second quarter wave plate. The efficiency of the

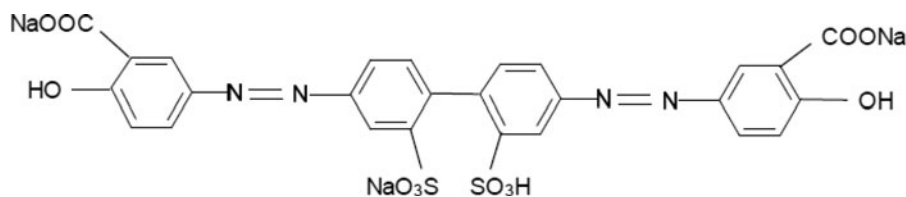


Figure 2. Structural formula of the mordant pure yellow dye.

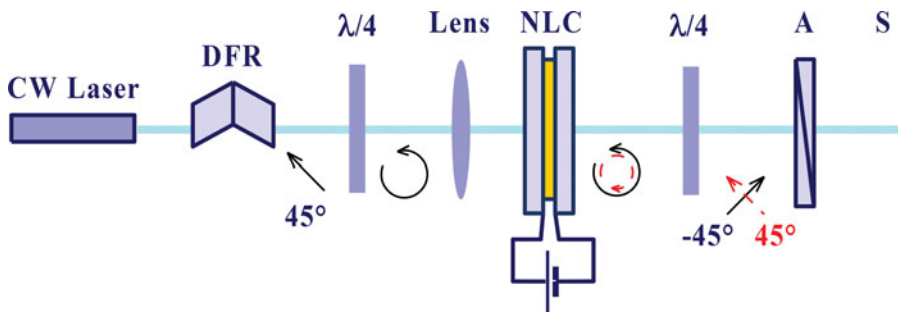


Figure 3. Experimental setup for the optical vortex generation in an NLC due to the photorefractive effect: (DFR) double Fresnel rhomb, ($\lambda/4$) quarter wave plates, (NLC) nematic liquid crystal cell, (A) polarizer-analyzer, and (S) screen. The distance from the NLC to the screen is 1 m. Arrows represent the polarizations of the non-vortex (solid curves) and vortex (dashed curves) components.

conversion with respect to the incident beam power is about 10% lower due to the reflection from the NLC cell interfaces.

Results and discussion

When the NLC was illuminated by the linearly polarized light beam, a pattern shaped as cross was observed in crossed polarizers. Such pattern suggests an axially symmetric director distribution, which is necessary for the vortex generation. It was observed for the samples with both the positive (Fig. 4a) and negative (Fig. 5a) dielectric anisotropy. The dc voltage required for the formation of distinguishable pattern was $U = 1.0$ and 4.5 V for ZhKM-1277 and F-3 nematic materials, respectively. This corresponds to the difference in the dielectric anisotropy of these materials.

Illumination of the samples subjected to dc voltage with the circularly polarized beam results in the appearance of the vortex component characterized by the circular polarization of the opposite sense. When the analyzer was crossed with the direction of the linear polarization of the non-vortex component, a ring typical of the vortex component was clearly seen (Figs. 4b and 5b). The corresponding patterns for the non-vortex components are presented in Figs. 4f and 5f.

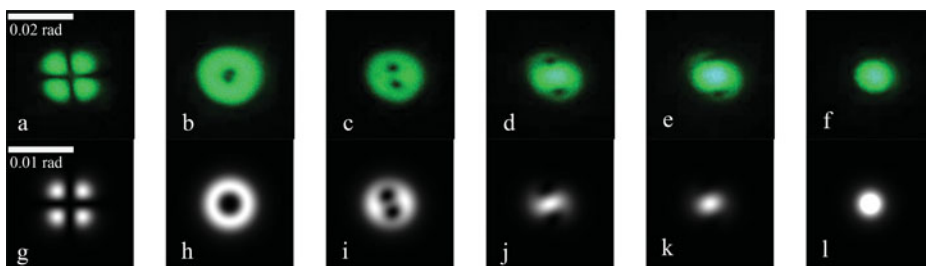


Figure 4. ((a)–(f)) Diffraction patterns in the cross section of the light beam ($P = 28$ mW) passed through homeotropic NLC ZhKM-1277 with positive dielectric anisotropy for different angles β of the analyzer rotation with respect to the vertical plane: (a) $\beta = -45^\circ$, without $\lambda/4$ plates; (b) $\beta = +45^\circ$ (the vortex component alone); (c) $\beta = +35^\circ$; (d) $\beta = +5^\circ$; (e) $\beta = -15^\circ$; (f) $\beta = -45^\circ$ (the non-vortex component alone). A dc voltage of 2.0 V is applied to the NLC cell. The conversion efficiency of the Gaussian beam to the vortex is about 5%. The angular size of the frames is 0.04 rad. ((g)–(l)) Corresponding diffraction patterns simulated according to Eqs. (2) and (3). The adjustable parameters in (3) are $a = 0.05$ and $b = 0.6$. The analyzer orientations are the same as in the upper row ((a)–(f)). The angular size of the frames is 0.02 rad.

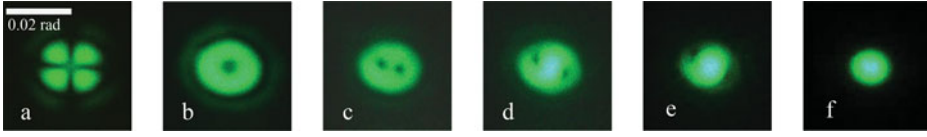


Figure 5. Diffraction patterns in the cross section of the light beam ($P = 12$ mW) passed through homeotropic NLC F-3 with negative dielectric anisotropy for different angles β of the analyzer rotation with respect to the vertical plane: (a) $\beta = -45^\circ$, without $\lambda/4$ plates; (b) $\beta = +45^\circ$ (the vortex component alone); (c) $\beta = +47^\circ$; (d) $\beta = +49^\circ$; (e) $\beta = 53^\circ$; (f) $\beta = -45^\circ$ (the non-vortex component alone). A dc voltage of 5.2 V is applied to the NLC cell. The conversion efficiency of the Gaussian beam to the vortex is about 1%. The angular size of the frames is 0.04 rad.

Intermediate orientations of the analyzer allowed the observation of the interference of the components. A characteristic S-shaped interference pattern (Figs. 4d and 5d) indicates the optical charge of the vortex equal to 2. The appearance of the pattern depends on the ratio of the intensities of the non-vortex and vortex components, which can be adjusted by rotating the analyzer. Better interference pattern is observed for comparable intensities.

The nonlinear phase shift S increases as the beam power increases. This is manifested in a more developed diffraction pattern with noticeable additional rings of the vortex beam (Fig. 6a) and pronounced helical structure of the interference pattern (Fig. 6b).

The diffraction patterns were simulated using a simple model of the nonlinear phase shift profile

$$S(u) = akL\Delta nu^2 e^{-bu^2}, \quad (3)$$

where a and b are adjustable parameters. Parameters a and b were fitted to obtain the best correspondence of the simulated and experimental patterns at the given conversion efficiency. The results of simulation ((g)–(l) in Fig. 4) show the qualitative agreement with experiment in the intensity profiles; however the beam divergence proved to be two times smaller than the experimental one. A more rigorous calculation requires a determination of the director distribution in the electric field of the light induced charges.

The efficiency η of the Gaussian beam to vortex conversion depends on the sign of dielectric anisotropy, NLC cell thickness, and experimental conditions such as applied voltage and the power and waist of the beam. In particular, it increases monotonically with the applied voltage. For ZhKM-1277 sample, the efficiency η increases from 1% at $U = 1.0$ V to 17% at $U = 3.5$ V. For F-3 sample, $\eta < 1\%$ and 32% at $U = 4.5$ and 6.0 V, respectively.

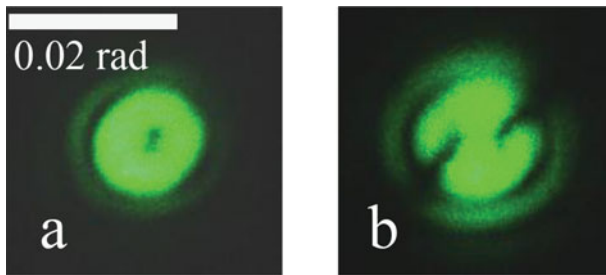


Figure 6. Diffraction patterns in the cross section of the light beam ($P = 26$ mW) passed through homeotropic NLC F-3 with negative dielectric anisotropy for different angles β of the analyzer rotation with respect to the vertical plane: (a) $\beta = +45^\circ$ (the vortex component alone) and (b) $\beta = +49^\circ$ (interference of the components). A dc voltage of 5.2 V is applied to the NLC cell. The angular size of the frames is 0.04 rad.

It should be noted that the pattern is not stable at high voltages. At $U > 5.5$ V, the pattern obtained with the F-3 sample becomes diffuse and distorted. This suggests the destruction of axially symmetric director distribution. For the ZhKM-1277 sample, the conversion efficiency decreases with time at $U > 2.5$ V.

It is likely that the stability of the director distribution in the case of negative dielectric anisotropy can be improved by adding a high-molar-mass dye dopant, which induces the torque rotating the NLC director perpendicularly to the light field [13]. This torque would support the initial director orientation at the beam axis.

Thus we implemented the optical vortex generation based on the photorefractive effect in NLCs with both positive and negative dielectric anisotropy. It should be expected that optimization of the NLC parameters and experimental conditions will make it possible to obtain a more stable director deformation and more efficient conversion to optical vortex.

The authors are grateful to M.I. Barnik and V.N. Ochkin for helpful discussions. The study was supported by the Russian Science Foundation, project no. 14-12-00784.

References

- [1] Abramochkin, E. G., & Volostnikov, V. G. (2010). *Modern Optics of Gaussian Beams*, Fizmatlit: Moscow.
- [2] Desyatnikov, A. S., Kivshar, Y. S., & Torner, L. (2005). *Prog. Opt.*, 47, 291–391.
- [3] Marrucci, L., Manzo, C., & Paparo, D. (2006). *Phys. Rev. Lett.*, 96, 163905-1–163905-4.
- [4] Barboza, R., Bortolozzo, U., Clerc, M. G., Residori, S., & Vidal-Henriquez, E. (2015). *Adv. Opt. Photonics*, 7, 635–683.
- [5] Brasselet, E., Murazava, N., Misawa, H., & Juodkazis, S. (2009). *Phys. Rev. Lett.*, 103, 103903-1–103903-4.
- [6] Brasselet, E. (2009). *Opt. Lett.*, 34, 3229–3231.
- [7] Budagovsky, I. A., Zolot'ko, A. S., Korshunov, D. L., Smayev, M. P., Shvetsov, S. A., et al. (2015). *Opt. Spectrosc.*, 119, 280–285.
- [8] Barboza, R., Bortolozzo, U., Assanto, G., Vidal-Henriquez, E., Clerc M. G. et al. (2012). *Phys. Rev. Lett.*, 109, 143901-1–143901-5.
- [9] Barboza, R., Bortolozzo, U., Assanto, G., & Residori, S. (2013). *Mol. Cryst. Liq. Cryst.*, 572, 24–30.
- [10] Budagovsky, I. A., Zolot'ko, A. S., Smayev, M. P., & Shvetsov, S. A. (2015). *Bull. Lebedev. Phys. Inst.*, 42, 319–322.
- [11] Pagliushi, P., & Cipparrone, G. (2004). *Phys. Rev. E*, 69, 061708-1–061708-7.
- [12] Budagovsky, I. A., Zolot'ko, A. S., Smayev, M. P., & Barnik, M. I. (2010). *JETP*, 111, 135–145.
- [13] Budagovsky, I. A., et al. (2011). *Polym. Sci., Ser. A*, 53, 655–665.